# Simulation of Shell-and-Tube Heat Exchanger as a Vapor Control Unit with different baffle angle

**Nattha Kanlayaprasit[1], Nattadon Pannucharoenwong[1*], Phadungsak Rattanadecho[1], Ponthep Vengsungnle[2]**

[1] Department of Mechanical Engineering, Faculty of Engineering, Thammasat University, Thailand
[2] Department of Agricultural Machinery Engineering, Faculty of Engineering and Architecture, Rajamangala University of Technology Isan, Thailand.
*Corresponding author. E-mail: pnattado@engr.tu.ac.th

## ABSTRACT

The transient behavior of heat exchangers has a dominant impact on the effectiveness of heat transfer in time-dependent thermal systems, especially in financial-limited scenarios and rapid heat sources. The present paper provides computational fluid dynamic (CFD) simulation for 2D model of shell-and-tube heat exchanger (STHE) in Ansys rendered environment. The tested 1200 mm in length STHE prototype consists of 2 baffles, 14 tubes with shell inside and tube outside diameter of 600 mm and 51 mm. In this simulation, the effect of baffle angles on outlet temperature of cold flow ($T_{C,out}$), log mean temperature, pressure drop in the cold domain and hot domain were examined. Simulation of three different baffle angles (70, 80, 90˚) revealed that the $T_{C,out}$ was slightly changed and pressure drop in cold and hot domain were quite significant. The log mean temperature difference resulted from alteration of baffle angles from 90 to 70˚ were 91.26, 91.27, and 91.31 K, respectively. From this log mean temperature difference, the overall heat transfer coefficient at baffle angles of 90, 80 and 70˚ were 0.8678, 0.8680 and 0.8700 kW/m$^2$K, respectively. The results demonstrated that using 70$^o$ baffle angle can achieve the highest heat transfer efficiency from the largest the LMTD and the overall heat transfer of the heat exchanger. The thermo-hydraulic performance of modeled heat exchanger from the simulation suggested that it can be used instead of the vapor recovery unit (VRU) that is currently employed in petroleum refineries.

**Keywords:** Computational fluid dynamic, Heat exchanger, Baffle angle, Vapor recovery unit

## 1. INTRODUCTION

Petroleum industry in Thailand has grown tremendously over the past few years due to globalization and increase in population. One of the major concerns regarding this industry is its negative impact on the environment and the ecosystem surrounding the establishment. McKee RH. et al. [1] and Hadidi et al. [2] Vapor recovery unit (VRU) was used to turn rich gas and distillate from the fluid catalytic cracking unit (FCCU) into liquefied petroleum gas and gasoline. In addition to having economic value, a vapor recovery unit also helps mitigate emission of toxic gas such as benzene, nitrogen oxide ($NO_x$), sulfur oxide ($SO_x$) and volatile organic compound (VOC). However, Webb G. [3] and Lu E. et al. [4] the current vapor recovery unit is expensive and requires high maintenance cost. Among various recovery installations, such as Shin MS. et al. [5] membrane, Ma H. et al. [6] extraction and Kosgey KE. et al. [7] mechanical vapor compression, applied heat exchanger have

Received 01-07-2019
Revised 16-09-2019
Accepted 20-09-2019

emerged as a promising technique and attracted remarkable attention due to its economic advantages compared with conventional VRU.

Yang J. et al. [8] and Markowski M. et al. [9] Shell-and-tube of heat exchanger (STHE) is usually employed due to its flexibility, toughness, and consistent performance. You Y. et al. [10] Baffle is a necessary component inside the heat exchanger due to their ability to increase the nusselt number, which reflects in the improvement of heat transfer performance. However, addition of baffles has a significant impact on pressure drop. Ambekar AS. et al. [11] have investigated the effect of four different baffle configurations on pressure drop inside the STHE and suggested that a double segmental baffle is better than single segmented. A helical baffle can reduce the pressure drop even further by more than roughly 30%. A finned type tube was also proposed to improve the heat transfer performance. Sadeghianjahromi A. et al. [12] successfully enhanced heat transfer using louver angle. The optimized louver angle found through genetic algorithm was $21^{o}$. In the cases, simulation of heat exchanger devices has been conducted in various research in order to determine the appropriate size of the device. Biglarian H et al. [13] reported mathematical modelling of borehole heat exchanger used as ground heating source for heat pump systems. In this report the length of the borehole was reduced by 16% due to appropriate simulation using Fluent software. Rahimi A. et al. [14] Fluid dynamic in terms of Rayleigh number was found to have a significant effect on heat transfer of C-shaped heat exchangers.

This Research aims to investigate the effect of baffle angle (70, 80 and 90˚) on log mean temperature, outlet temperature, pressure drop in both cold and hot domains. A computational fluid dynamic analysis of the modeled STHE will be used to generate temperature profile and vector profile of fluid dynamic in an operating heat exchanger. A successful prototype will be installed to recover the emission of vapor from the refining unit in the petroleum industry.

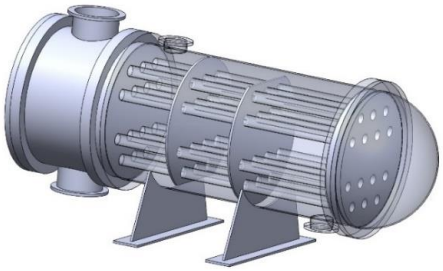

**Figure 1.** 3D view of the shell and tube heat exchanger designed.

## 2. EXPERIMENTAL METHOD

2.1 Governing equation

Based on Çengel YA. et al. [15] The analysis of the continuous steady state -, Versteeg HK. et al. [16,17] and Pozrikidis C. et al. [18] including of energy balance (4) is shown in equation (1) to equation (4). The parameters used to calculate these equations are shown in Table 1.

**Table 1.** Mathematical operating conditions employed to heat exchanger analysis.

| Level | Conditions |
|---|---|
| 1 | Analysis of steady state system |
| 2 | Use properties of water for analysis of fluid at high and low temperature. |
| 3 | Three-dimensional analysis |
| 4 | Analysis included gravity |
| 5 | Using standard k-epsilon to simulate viscosity |
| 6 | Solve pressure-velocity coupling by simple scheme |

Continuity: $$\frac{\partial \rho}{\partial t} + div(\rho u) = 0 \quad (1)$$

x-momentum: $$\frac{\partial(\rho u)}{\partial t} + div(\rho u u) = -\frac{\rho p}{\partial x} + div(\mu grad u) + S_{Mx} \quad (2)$$

y-momentum: $$\frac{\partial(\rho v)}{\partial t} + div(\rho v u) = -\frac{\rho p}{\partial y} + div(\mu grad v) + S_{My} \quad (3)$$

z-momentum: $$\frac{\partial(\rho w)}{\partial t} + div(\rho w u) = -\frac{\rho p}{\partial z} + div(\mu grad w) + S_{Mz} \quad (4)$$

Friction factor (f) can be used to calculate pressure drop (ΔP) which can be found through equation (5), given length (L), average velocity (v), $\rho$ is the density of fluid and inside diameter ($d_i$).

$$\frac{\Delta P}{\rho} = f \frac{L}{d_i} \frac{V^2}{2} \quad (5)$$

Heat power emitted and absorbed are found using the equation below. The two values of heat can then be used to calculate the efficiency ($\eta$) of the heat transfer device.

$$\dot{Q}_H = \dot{m}_H C_{P,H}(T_{H,in} - T_{H,out}) \quad (6)$$

$$\dot{Q}_C = \dot{m}_C C_{P,c}(T_{C,out} - T_{C,in}) \quad (7)$$

$$\eta = \frac{\dot{Q}_C}{\dot{Q}_H} \times 100\ \% \quad (8)$$

Log mean temperature can be found by measuring the temperature of hot and cold flow both into and out of the heat exchanger.

$$\Delta T_1 = T_{H,in} - T_{C,out}$$
$$\Delta T_2 = T_{H,out} - T_{C,in}$$
$$\Delta T_{lm} = \frac{\Delta T_1 - \Delta T_2}{ln\,(\Delta T_1 - \Delta T_2)} \quad (9)$$

Overall heat transfer coefficient:

$$\frac{1}{U} = \frac{1}{h_o} + \frac{1}{h_{od}} + \frac{d_o\ ln\ ln\left(\frac{d_o}{d_i}\right)}{2k_w} + \frac{d_o}{d_i h_i} + \frac{d_o}{d_i h_{id}} \quad (10)$$

Where
$U_o$ = Overall heat transfer coefficient ($W/m^2K$),
$h_o$ = Outside fluid film coefficient ($W/m^2K$),
$h_i$ = Inside fluid film coefficient ($W/m^2K$),
$h_{od}$ = Outside fouling factor coefficient ($W/m^2K$),
$h_{id}$ = Inside fouling factor coefficient ($W/m^2K$),
$k_w$ = thermal conductivity of tube wall material(W/mK),
$d_i$ = Tube inside diameter (m),
$d_o$ = Tube outside diameter (m)

Rate of net heat transfer: $$\dot{Q} = \dot{m} c_p \Delta T + \dot{m} L = A U_o \Delta T_{lm} \quad (11)$$

Where
$Q_{dot}$ = Rate of net heat transfer (kJ/s),
$\dot{m}$ = Mass flow rate (kg/s),
$c_p$ = Specific heat of substance (kJ/kg·K),
L = Latent heat of substance (kJ/kg),
$U_o$ = Overall heat transfer coefficient ($W/m^2$·K),
$\Delta T_{lm}$ = Log mean temperature (K)

The velocity (v) can be found using equation 12 given mass flow rate (ṁ), Density of substance (ρ) and Tube inside diameter ($d_i$).

$$v = \frac{\dot{m}}{\frac{\pi}{4}\rho d_i^2} \quad (12)$$

2.2 Design of a shell and tube heat exchanger

The parameters used to calculate these equations are shown in Table 1. The first step is to analyze by assuming that the system is in steady state condition. The properties of water such as density and vapor pressure were then plugged into the software considering both high and lower temperature fluid. Three-dimensional analysis of the heat exchanger system was then performed including gravity and standard k-epsilon to simulate viscosity. The pressure-velocity coupling equation was then solved using the simple scheme. The operating condition and basic configuration of the heat exchanger are shown in Table 2.

**Table 2.** Geometric design inside the heat exchanger.

| Designation | Value/Unit |
|---|---|
| Baffle cut | 25% |
| Heat exchanger length | 1,200 mm |
| Working fluid | Water |
| Inlet & outlet shell nozzle diameter | 96 mm |
| Number of Baffles | 2 |
| Number of tubes | 14 |
| Shell inside diameter | 600 mm |
| Tube outside diameter | 51 mm. |
| Baffle Space | 300 mm |

In Figure 2, the heat exchange is composed of channel nozzle (inlet and outlet), shell nozzle (inlet and outlet), shells, tubes and a shell cover as shown in Figure 2a. Figure 2b depicted the circular plate or the baffle used to hold the tubes in their places.

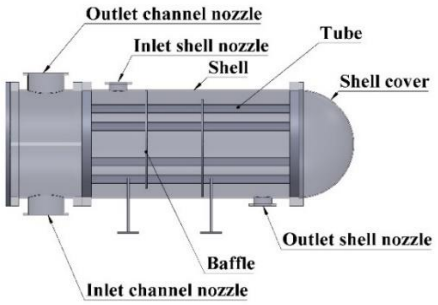


(a)

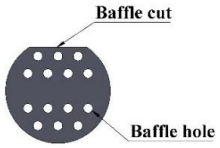


(b)

**Figure 2.** Typical parts of heat exchanger designed (a) and the baffle (b).

Figure 3 shows the operating procedure of the heat exchanger with varied parameters as shown in Table 3. Cold water will enter the inlet channel nozzle and then circulate along each tube, into the shell cover and then exit at the outlet channel nozzle located at the top of the heat exchanger. Similarly, hot water is set into the inlet shell nozzle, while then flow to the shell parallel with the baffle, through the baffle cut and then out through the outlet shell nozzle.

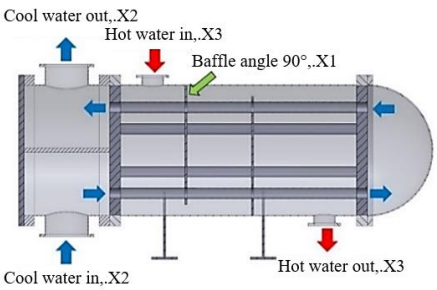


**Figure 3.** General operation of a heat exchanger.

Comparison of heat transfer capability at different as baffle angle changes were conducted. This test was performed to compare the ability of heat exchange devices at different baffle angles according to the parameters as shown in Table 3.

**Table 3.** Parameters for analysis of heat exchanger.

| Parameter/Abbreviation | Value/Unit |
|---|---|
| Baffle angle, X1 | 90,80,70º |
| Rate of cooled water, X2 | 4 L/s |
| Rate of hot water, X3 | 30 L/s |
| Temperature of cold water, X4 | 300 K |
| Temperature of hot water, X5 | 400 K |

## 3. RESULTS AND DISCUSSION

Results from the computational dynamic fluid analysis on the operating heat exchanger are shown in Figure 4 to 7. Figure 4 (a) demonstrated the front view analysis showing the effect of temperature when the baffle angle was set at 90º. A reduction of baffle angle from 90º to 70º was found to have an insignificant effect on the temperature distribution of the operating heat exchanger.

Figure 5a-c demonstrated the side view analysis of the effect of temperature at different baffle angles. The side view demonstrates also indicated that the baffle angle has insignificant effect on the temperature profile inside the heat exchanger.

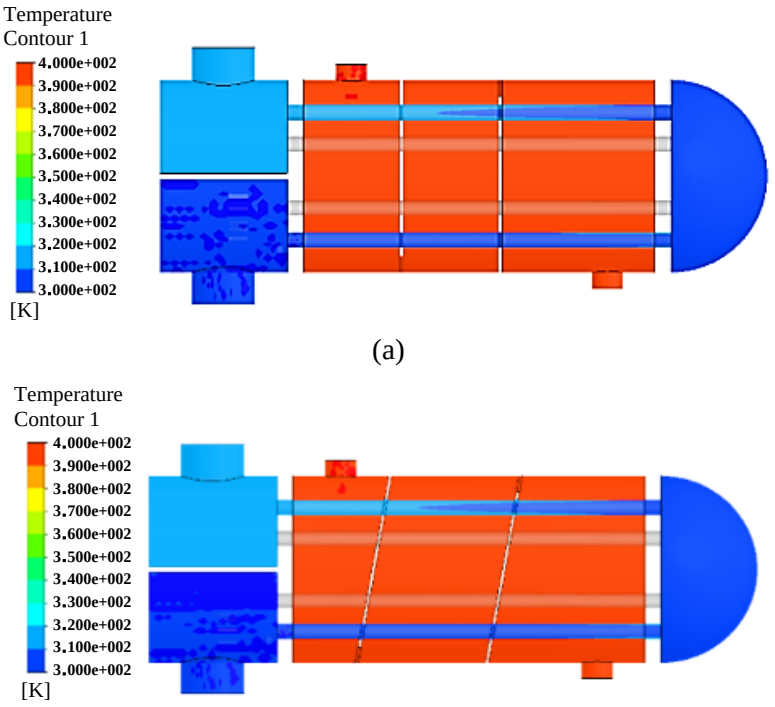


**Figure 4.** Front view contour of temperature of fluid in front baffle angle 90º (a), 80º (b) and 70º(c).

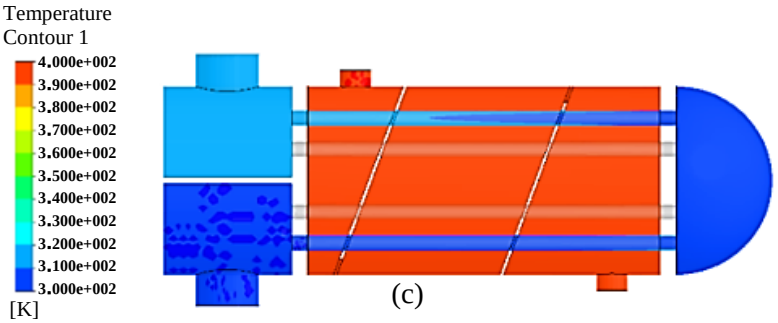


**Figure 4.** (Continue) Front view contour of temperature of fluid in front baffle angle 90º (a), 80º (b) and 70º(c).

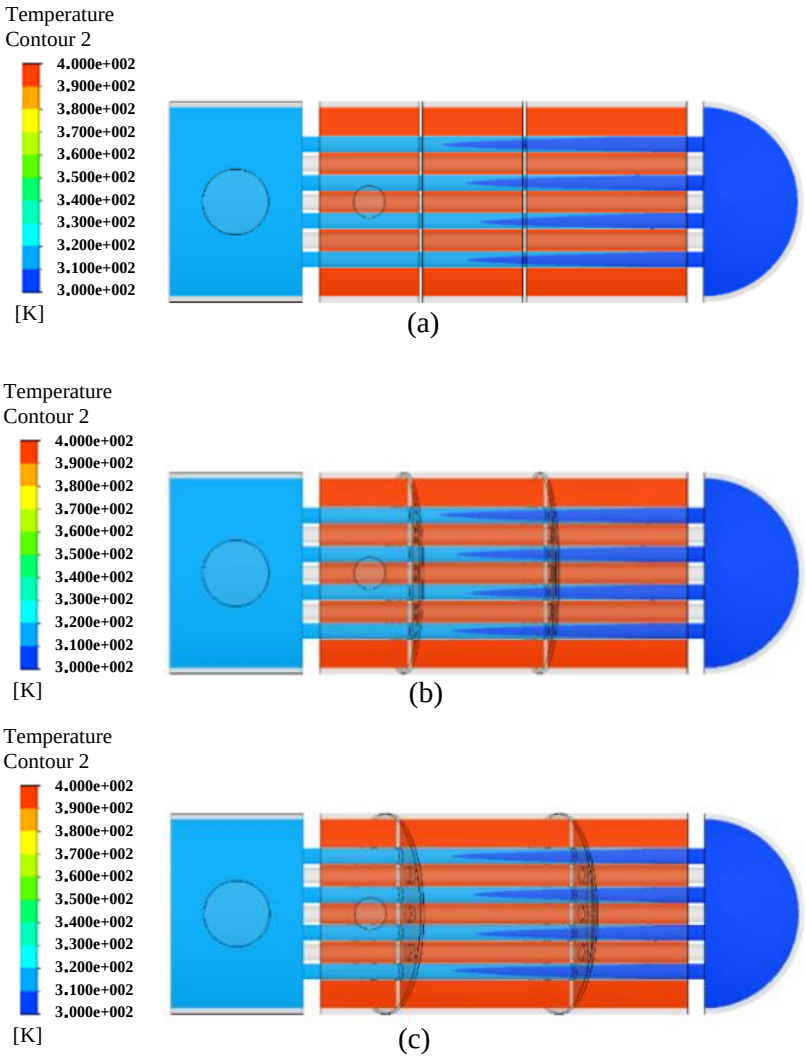


**Figure 5.** Side view contour of temperature of fluid in top baffle angle 90º (a), 80º (b) and 70º(c).

Formation of vortices were illustrated in the vector profile of fluid flow inside the heat exchangers shown in Figure 6 and 7. These vortices indicated intense mixing of the fluid implying turbulent behavior and rapid heat transfer. In Figure 6 (a), revealed formation of several vortices along the length and the shell cover of the heat exchanger with 90$^{o}$ baffle angle. A reduction in baffle angle to 80$^{o}$ caused formation of another vortex located at the outlet of cool water as shown in Figure 6b. However, when the baffle angle was reduced further to 70$^{o}$ the vortices along the tubes started to disappear, only the vortex at the shell cover remained.

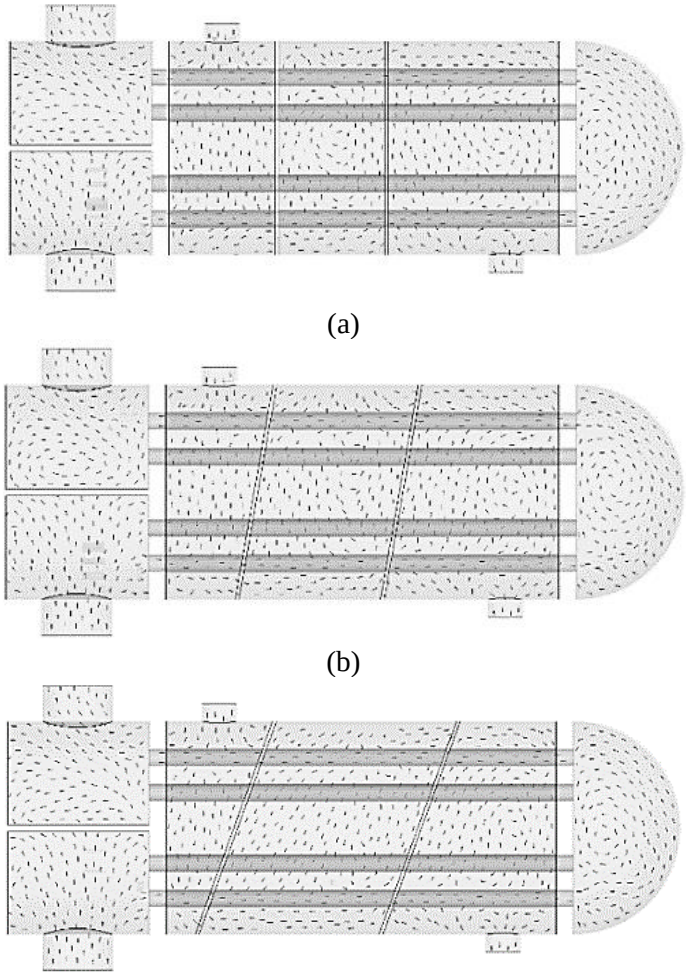

(a)

(b)

(c)

**Figure 6.** Top view vector of flow at different simulated baffle angle 90º (a), 80º (b) and 70º(c).

Figure 7 demonstrated the side view perspective of the vector profile inside the heat exchanger. Table 4 show the calculated value of temperature and pressure drop at different locations of the heat exchanger.

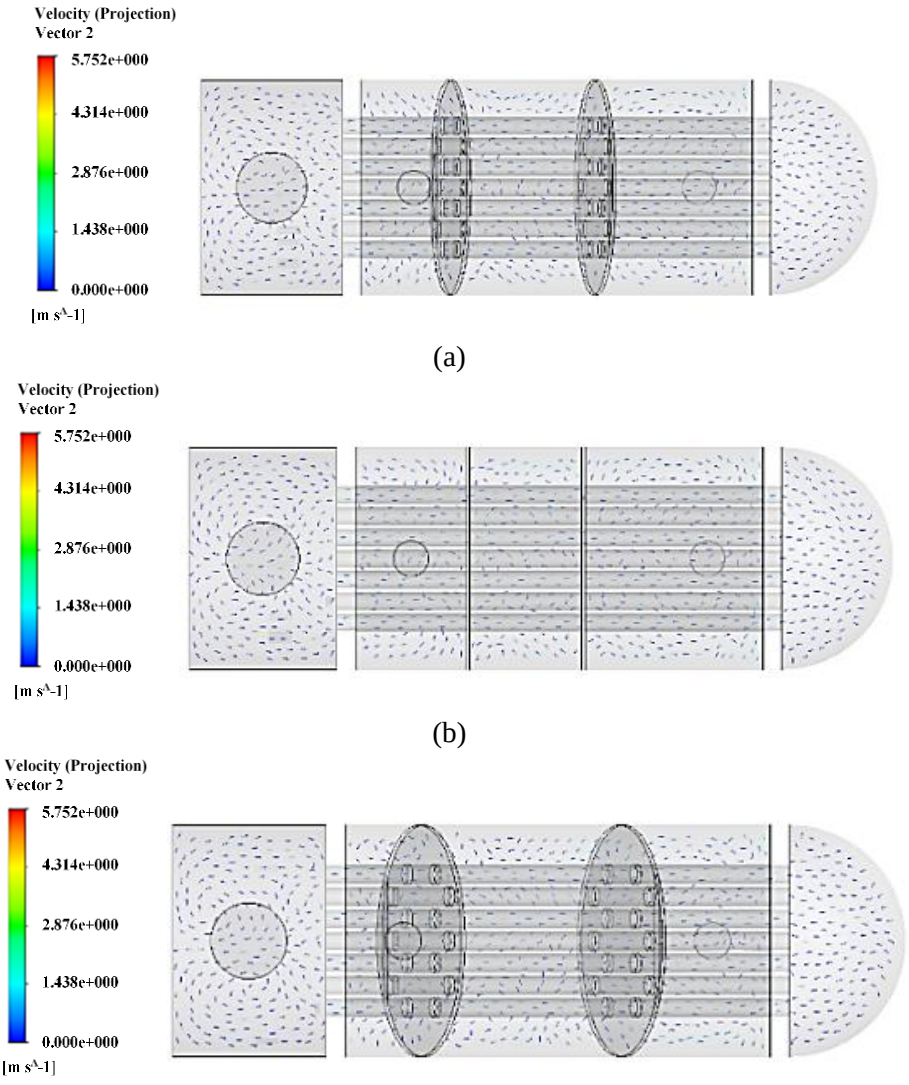


**Figure 7.** Side view vector of flow at different simulated baffle angle 90º (a), 80º (b) and 70º (c).

**Table 4.** Comparative analyses of changes in baffle angle.

| Level | Parameter | Baffle angle (°) | | | Unit |
|---|---|---|---|---|---|
| | | 70 | 80 | 90 | |
| 1 | Pressure drop | 426 | 429 | 422 | Pa |
| 2 | Highest temperature of cold water | 320 | 320 | 320 | K |
| 3 | Average temperature of cold water | 307 | 307 | 307 | K |
| 4 | Inlet temperature of cold water | 300 | 300 | 300 | K |
| 5 | Outlet temperature of cold water | 314 | 314 | 314 | K |
| 6 | Highest speed of cold water | 0.598 | 0.5863 | 0.5919 | m/s |
| 7 | Average speed of cold water | 0.1632 | 0.1657 | 0.1642 | m/s |
| 8 | Highest pressure of cold water | 409 | 414 | 405 | Pa |
| 9 | Average pressure of cold water | 176 | 181 | 174 | Pa |
| 10 | Highest temperature of hot water | 400.00 | 400 | 400 | K |
| 11 | Average temperature of hot water | 397 | 397 | 398 | K |
| 12 | Inlet temperature of hot water | 400.00 | 400.00 | 400 | K |
| 13 | Outlet temperature of hot water | 397 | 397 | 397 | K |
| 14 | Highest speed of hot water | 5.8572 | 5.6285 | 5.6335 | m/s |
| 15 | Average speed of hot water | 0.7164 | 0.7172 | 0.7210 | m/s |
| 16 | Highest pressure of hot water | 32,964 | 56,562 | 26,721 | Pa |
| 17 | Pressure of cold water | 13,799 | 38,360 | 9,530 | Pa |

Comparison of pressure and temperature calculated at different parts of the heat exchanger were demonstrated in Figure 8 to 11. According to Figure 8, pressure drop along the cold-water domain was found to increase as baffle angle increases from 90° to 80° and then reduced again as the baffle angle increases to 70°.

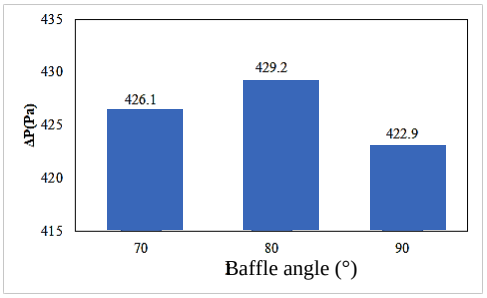


**Figure 8.** Pressure drop-in cold-water domain.

The average speed of was the highest at a baffle angle of 80°, followed by 90° and then 70° (Figure 9). This suggested that if the average speed is too high then the system risked having high pressure drop.

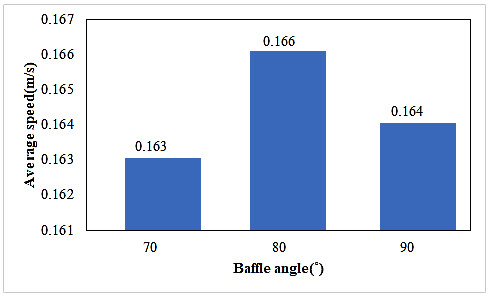


**Figure 9.** Average speed of cold-water domain.

Figure 10 reveales the averaged pressure of the cold-water domain.

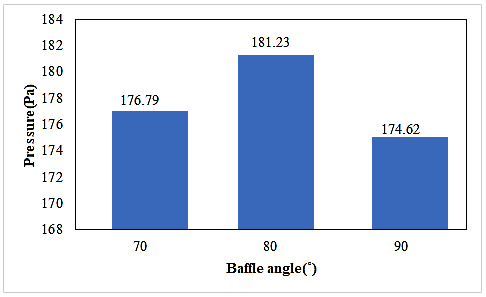


**Figure 10.** Average pressure cold water domain.

The outlet temperature of cold water was the highest at baffle angle of 90° as shown in Figure 11.

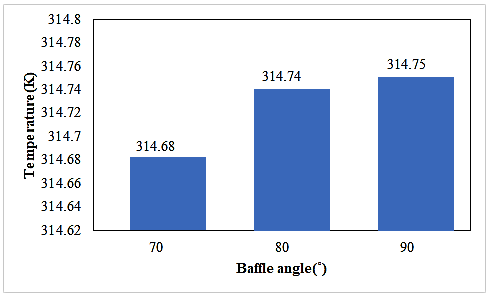


**Figure 11.** Outlet temperature of cold water.

The simulation results of outlet cold water shown in Figure 11 substituted in equation (9), which gave log mean temperature difference as shown in Figure 12. It can be observed that the heat exchanger with 70° baffle angle gave the highest long mean temperature difference compared with other baffle angles and indicated the most effective heat transfer.

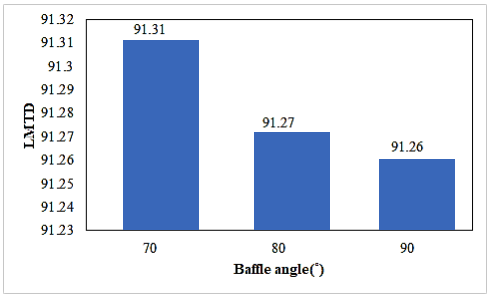


**Figure 12.** Log Mean Temperature Difference (LMTD).

Figure 13 shows the pressure drop of hot water at different baffle angles. Simulation results show that pressure drop was the highest at the baffle angle of 80°, followed by 70° and then 90°.

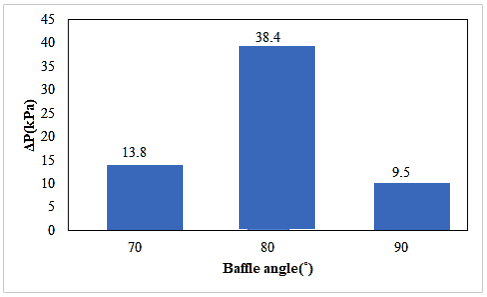


**Figure 13.** Pressure drop of hot domain.

As shown in Figure 14 relevant research on heat exchanger simulation by Bin Gao also suggested a proportional relationship between baffle angle and pressure drop as shown in Figure 14. [19]. However, unlike this work their research does not include a baffle angle of 90°.

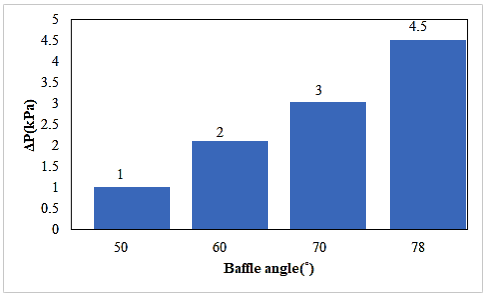


**Figure 14.** Pressure drop in hot water from Gao B.'s journal [19].

This is because the temperature difference between the inlet and outlet temperature of the heat exchanger with 70° baffle angle is the largest calculated from equation 9. The over heat transfer coefficient of baffle angles 90°, 80° and 70° are 0.8678, 0.8680 and 0.8700 kW/m$^2$K, respectively.

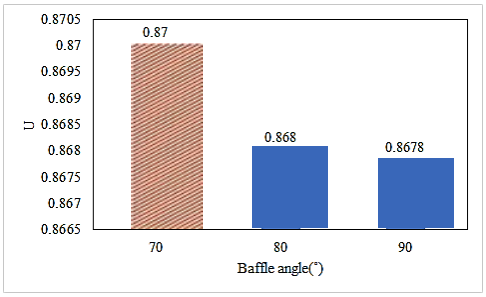


**Figure 15.** Overall Heat Transfer Coefficient, U.

Figure 16 shows the efficiency of heat transfer inside the heat exchanger at different baffle angles, which are calculated using equation (8). It can be found that the heat transfer efficiency of a heat exchanger with 70° baffle angle is the highest compared with heat transfer efficiency of heat exchanger with 80° and 90°, respectively.

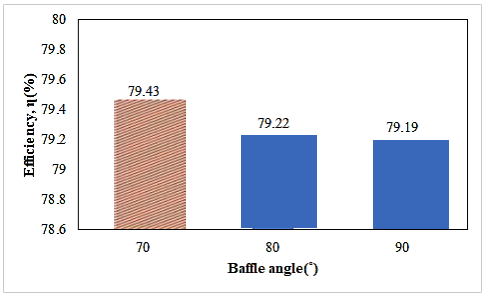


**Figure 16.** Efficiency of heat transfer inside the heat exchanger.

## 4. CONCLUSION

In this study, using computational fluid dynamic analysis is a comparison of heat transfer capability at different baffle angle changes. From analysis results, demonstrate the effect of temperature and cold-water parameters. The outlet temperature of cold water 90° baffle angle is 314.753K higher than with 80° and 70° baffle angles, respectively. As the baffle angle was varied from 90 to 70°. Pressure drop inside hot domain, variation of the average pressure for cold water, the pressure drop in cold water with 80˚ baffle angle is the largest because of the fastest velocity. However, the heat transfer efficiency using 70° baffle angle is the highest indicating optimized heat transfer capability because the LMTD and the overall heat transfer of the heat exchanger are the largest than another baffle angle. It can be concluded that the 70° baffle angle presents the best comprehensive performance among the baffle angle of heat exchangers prototype to replace the vapor recovery unit (VRU) for PTT Co. Ltd.

## 5. ACKNOWLEDGEMENTS

The researchers would like to thank the Petroleum Authority of Thailand Phra Khanong which supported us with the facilitated research in this and this research was supported by the Faculty of Engineering Research Fund, Thammasat University. And also, Tokyo Institute of Technology for providing useful information.

## 6. REFERENCES

[1] McKee RH, Trimmer GW, Whitman FT, et al. Assessment in rats of the reproductive toxicity of gasoline from a gasoline vapor recovery unit. Reprod Toxicol. 2000; 14(4):337-53.

[2] Hadidi LA, AlDosary AS, Al-Matar AK, et al. An optimization model to improve gas emission mitigation in oil refineries. Journal of Cleaner Production. 2016; 118:29-36.

[3] Webb G. Ensuring effective vapour recovery in oilfield storage. World Pumps. 2017; 2017(1):14-16.

[4] Lu E, Zhang H, Zhu Z. A novel design for vapor recovery units. Comput Chem Eng. 2000; 24(2):1317-22.

[5] Shin MS, Jeon YW. Effect of membrane selectivity and partial pressure on vapor removal and sensible heat recovery in membrane

processes. Energy Procedia. 2017; 136:323-29.
[6] Ma H, Yu G, She Y, et al. A parabolic solvent chamber model for simulating the solvent vapor extraction (VAPEX) heavy oil recovery process. J Petrol Sci Eng. 2017;149:465-75.
[7] Kosgey KE, Kiambi SL, Cherop PT. Analysis of potassium nitrate purification with recovery of solvent through single effect mechanical vapor compression. S Afr J Chem Eng. 2017; 24:1-7.
[8] Yang J, Fan A, Liu W, et al. Optimization of shell-and-tube heat exchangers conforming to TEMA standards with designs motivated by constructal theory. Energ Convers Manag. 2014; 78:468-476.
[9] Markowski M, Trafczynski M, Urbaniec K. Identification of the influence of fouling on the heat recovery in a network of shell and tube heat exchangers. Appl Energ. 2013; 102:755-64.
[10] You Y, Fan A, Lai X, et al. Experimental and numerical investigations of shell-side thermo-hydraulic performances for shell-and-tube heat exchanger with trefoil-hole baffles. Appl Therm Eng. 2013; 50(1):950-56.
[11] Ambekar AS, Sivakumar R, Anantharaman N, et al. CFD simulation study of shell and tube heat exchangers with different baffle segment configurations. Appl Therm Eng. 2016;108: 999-1007.
[12] Sadeghianjahromi A, Kheradmand S, Nemati H. Developed correlations for heat transfer and flow friction characteristics of louvered finned tube heat exchangers. Int J Therm Sci. 2018; 129:135-44.
[13] Biglarian H, Abbaspour M, Saidi MH. Evaluation of a transient borehole heat exchanger model in dynamic simulation of a ground source heat pump system. Energy. 2018;147:81-93.
[14] Rahimi A, Saee AD, Baghban A, et al. Double-MRT lattice Boltzmann simulation of natural convection in a C-shaped heat exchanger. Powder Tech. 2018;336:465-80.
[15] Çengel YA, Ghajar AJ. Heat and Mass Transfer. 5th ed. United States of America: McGraw-Hill Education; 2015.
[16] 3D Heat Transfer Simulation & Thermal Analysis Software. ARRK Corporation.
[17] Versteeg HK, Malalasekera W. An Introduction to Computational Fluid Dynamics. 2nd ed. England: Pearson Education Limited; 2007.
[18] Pozrikidis C. Introduction to Theoretical and Computational Fluid Dynamics. 2nd ed. New York: Oxford University Press, Inc.; 2011.
[19] Gao B, Bi Q, Nie Z, et al. Experimental study of effects of baffle helix angle on shell-side performance of shell-and-tube heat exchangers with discontinuous helical baffles. Exp Therm Fluid Sci. 2015; 68:48-57.